CLM-P733

CULHAM LABORATORY
LIBRARY
1 APR 1985

CLM-P733

UKAEA

Preprint

TRANSMUTATION AND ACTIVATION EFFECTS IN HIGH-CONDUCTIVITY COPPER ALLOYS EXPOSED TO A FIRST WALL FUSION NEUTRON FLUX

G. J. BUTTERWORTH

CULHAM LABORATORY
Abingdon Oxfordshire

1985

This document is intended for publication in a journal or at a conference and is made available on the understanding that extracts or references will not be published prior to publication of the original, without the consent of the authors.

Enquiries about copyright and reproduction should be addressed to the Librarian, UKAEA, Culham Laboratory, Abingdon, Oxon. OX14 3DB, England.

CLM-P 733

TRANSMUTATION AND ACTIVATION EFFECTS IN IN HIGH-CONDUCTIVITY COPPER ALLOYS EXPOSED TO A FIRST WALL FUSION NEUTRON FLUX

G J Butterworth

Culham Laboratory, Abingdon, Oxon OX14 3DB

(UKAEA/Euratom Fusion Association)

Abstract

Transmutation and activation characteristics are calculated for a number of high-conductivity copper-based alloys exposed to 2.5 years continuous irradiation in the first wall neutron flux of the Culham Conceptual Tokamak Reactor IIA with neutron power loading of 7 MWm^{-2}. The computations are based on a modified form of the ORIGEN code and the cross section data library UKCTRIIIA. It is found that the copper base transmutes to other elements, principally nickel and zinc, at the rate of 0.28 weight percent per $MWym^{-2}$. The probable effect of these unintended alloying additions on the thermal conductivity is briefly discussed. Since their activities are generally dominated by that of the copper component, the dilute alloys studied exhibit very similar activation and decay properties. The long-term surface dose rate of alumina dispersion strengthened alloys may, however, be dominated by the γ decay of $^{26}A\ell$ with half life 7.4×10^5 y. Comparison is made with the activation characteristics of type 316 austenitic steel and the martensitic steel HT-9. It is noted that the long-term activity of copper alloys may in practice be governed by their silver impurity content, unless this can be reduced to about 1 ppm.

(Submitted for publication in Journal of Nuclear Materials)

February 1985

Transmutation and activation effects in high-conductivity copper alloys exposed to a first wall fusion neutron flux

by

G J Butterworth

Culham Laboratory, Abingdon, Oxon. OX14 3DB

Page 17 Line 19

. . . between 10 and 100 years . . . should read:

. . . between 100 and 1000 years

Page 18 Figure 12

The values indicated on the time axis are incorrect. These should range from 10^0 to 10^4 and not 10^{-1} to 10^3.

Please replace with the corrected figure below.

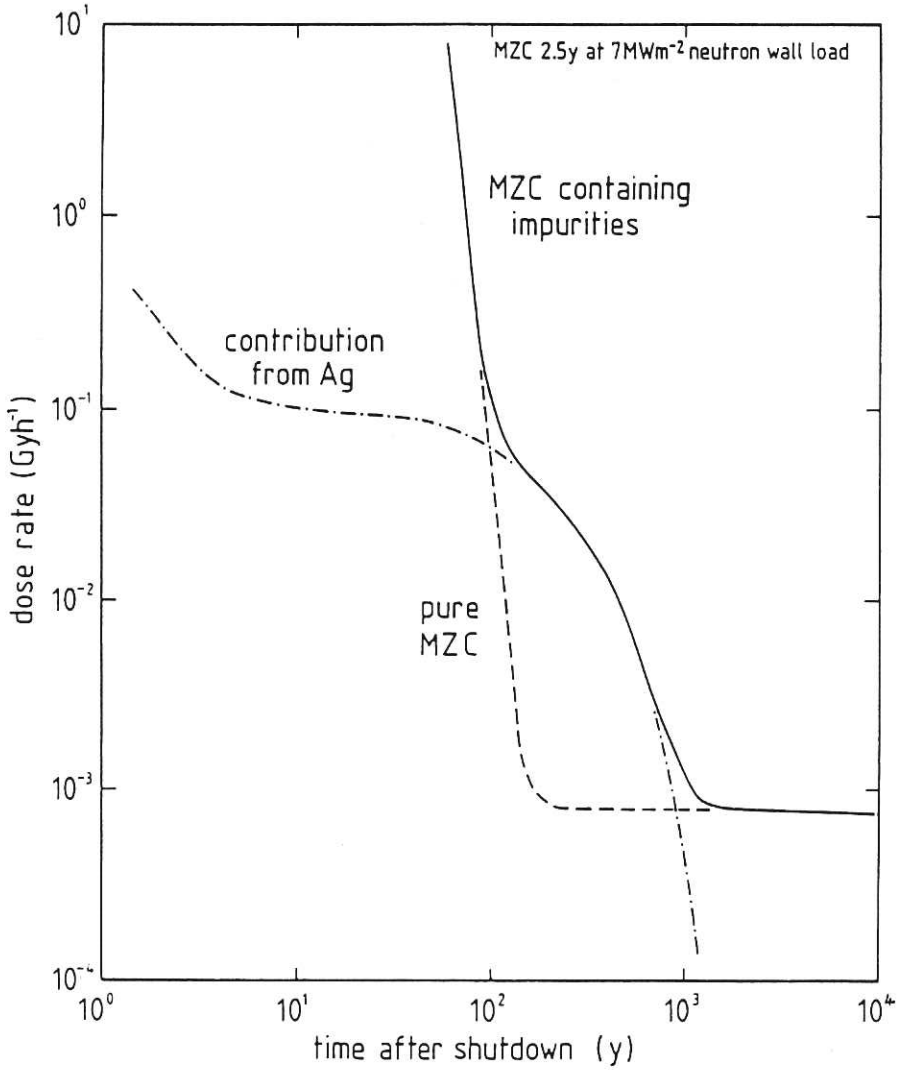

1. Introduction

Copper alloys in general and the high-conductivity coppers in particular appear attractive for use as fusion reactor first wall and limiter or divertor materials. Their high thermal conductivity not only facilitates heat transfer to the coolant but also reduces the thermal stressing which results in creep and thermal fatigue. A general assessment of the potential of high performance copper alloys as first wall materials has been made by Harling, Yu, Grant and Meyer[1] whilst Cort, Graham and Christensen[2] have examined the performance of a modular copper alloy first wall for a compact reversed-field-pinch reactor having a high wall loading and short-pulse operating mode. More recent thermal-hydraulic analyses of copper alloy first walls have been performed by Cooke and Krakowski[3] and by Caie and Butterworth[4]. As an example of the broader employment of these materials, a design proposed for the INTOR divertor uses a collector plate made from a refractory metal alloy to which is bonded a heat sink of copper or copper alloy.

The combination of high strength with high thermal conductivity is found in copper alloys containing only relatively low proportions of alloying additions, generally up to about 1% by weight. Such alloys can exhibit thermal conductivities around 80% that of pure copper[5]. Although higher concentrations of alloying additions may further enhance the mechanical properties they invariably reduce the thermal conductivity, hence the highly-alloyed compositions are of little interest for the present application.

In the hard first wall neutron spectrum the alloys will be subject to various nuclear reactions producing both gaseous and solid transmutation elements. It is to be expected that the progressive accumulation of these solid transmutation elements will exert a much more pronounced effect on the properties of the present compositionally-simple copper alloys than will the transmutations occurring in structurally-complex highly-alloyed materials such as stainless steels. It is therefore important to predict the transmutation rates and to evaluate the probable influence of the consequent changes in composition on the properties of the alloys. In addition, the results of the activation and decay calculations are of value in assessing the radiological implications associated with the use of copper alloys for first wall or blanket components and in identifying possible scenarios for their recycling or disposal.

2. Alloy compositions

The high-conductivity coppers may be classified into three groups:

(1) solid solution hardened alloys
(2) precipitation hardened alloys
(3) dispersion hardened alloys

The first group utilises solution hardening elements such as silver, cadmium and tin, which have minimal adverse effect on the conductivity but which strengthen the matrix, raise the softening temperature and increase the creep strength. Most of the commercial high-conductivity alloys fall within the second group. They derive their properties from the decomposition of a supersaturated solid solution at elevated temperature, which leads to the homogeneous precipitation of a second phase on a very fine scale. The most commonly employed strengthening elements are beryllium, chromium and zirconium. In the third group of alloys a pure copper matrix is strengthened with a dispersed oxide such as alumina or zirconia at a concentration up to about 1% by weight. With very fine oxide dispersions the resulting material is resistant to softening up to high temperatures and has excellent conductivity and creep strength.

The activities and surface dose rates induced by exposure to a first wall neutron flux have been calculated by Jarvis[6,7] for many of the stable elements. Using these results, the dose rates for copper and a number of elements commonly employed as alloying additions are compared in Fig.1. It is seen that chromium and magnesium give rise to relatively insignificant long-term dose rates in comparison with that of copper. Although the dose rate of zirconium is roughly a factor 10 higher than that of copper in the period 10^2 to 10^4 years after irradiation, its contribution to the total dose rate will be negligible in the case of high conductivity alloys, which contain typically less than 1% of zirconium. It will be noted, on the other hand, that after about 100 years the dose rate of aluminium is 10^3 times that of copper and persists at a high level for about 10^5 years. Thus even the modest concentrations of aluminium present in the alumina dispersion strengthened alloys may dominate their long term dose rates. Silver is employed as an alloying element in some high conductivity copper alloys and brazing materials and is, in any case, usually present as a principal impurity in commercial coppers. Because of its very high long-term dose rate, silver is particularly undesirable as an alloy constituent, even as an impurity at a level of a few parts per million. The influence of particular impurity elements such as silver on the activation properties of the alloys is discussed in a later section.

The nominal compositions of the alloys chosen for the present study are given in Table 1. In this table alloy A represents a casting composition containing a small proportion of beryllium in addition to chromium; B is a typical copper-chromium-zirconium alloy; C is a dispersion-strengthened alloy containing 0.38% Al_2O_3 and D a quaternary Cu-Cr-Zr-Mg

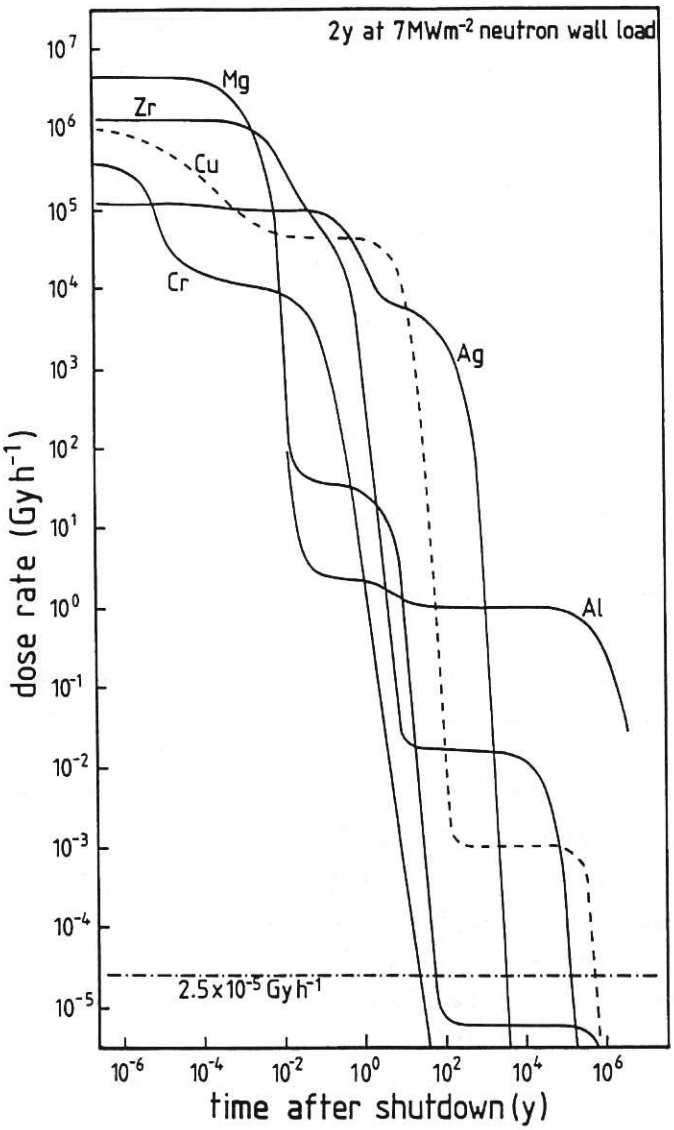

Figure 1 Comparison of the surface dose rates for the principal constituent and impurity elements in the alloys studied. The curves are from Ref. 6 and correspond to an exposure of the pure elements to a neutron power flux of 7 MWm^{-2} for 2 years.

Table 1
Nominal weight-percentage compositions of the selected alloys

Alloy	Cu	Be	O	Mg	Aℓ	Cr	Zr
A	99.1	0.10	–	–	–	0.80	–
B	99.5	–	–	–	–	0.30	0.20
C	99.6	–	0.18	–	0.20	–	–
D	99.2	–	–	0.05	–	0.60	0.20

precipitation-strengthened composition usually referred to as MZC.

3. Neutron flux and energy spectrum

For computational purposes the neutron flux and spectrum have been taken to be those at the first wall of the Culham Conceptual Tokamak Reactor Mark IIA[8], in which the time-averaged neutron power density is assumed to be 7 MWm^{-2}. Taking into account the energy gain from transmutations in the breeder material and assuming that all of the thermonuclear energy flux passes through the first wall, the above neutron power density corresponds to a total first wall power rating of 10 MWm^{-2}. In this reactor design the first wall is integral with the blanket. The structural material of the blanket is type 316 stainless steel, with liquid lithium as the breeder material and helium as the coolant. For the purpose of the calculation the blanket is modelled as a series of infinitely-long coaxial cylindrical zones with the azimuthal structure homogenised, as illustrated in Fig. 2. The neutron fluxes indicated in the figure represent the values at the centres of the various zones and are calculated from the one-dimensional transport code ANISN[9]. It is seen that the neutron flux of 2.44×10^{19} $m^{-2}s^{-1}$ is appreciably higher than the incident 14 MeV neutron current of 3.22×10^{18} $m^{-2}s^{-1}$; this is due to backscattering. The neutron energy spectra at several points in the blanket-shield region are depicted in Fig. 3. Whilst the calculation of the first wall flux and spectrum is based on a particular blanket model, it is found that the results are fairly insensitive to the choice of blanket materials[9]. The activation and transmutation calculations should therefore serve for at least a first order comparison of different first wall materials, irrespective of the particular blanket design.

The materials are assumed to be irradiated continuously for 2.5 years. This exposure corresponds to a neutron power fluence of 17.5 $MWym^{-2}$ (25 $MWym^{-2}$ total power fluence) and a neutron fluence, summed over all neutron energies, of 1.66×10^{27} m^{-2}. The resulting activation and transmutation effects are calculated with the aid of the neutron cross-section data library UKCTRIIIA[10] in conjunction with a modified form of the isotope generation and depletion code ORIGEN[11]. In general the results can be scaled to other wall loadings and irradiation times by noting that the activity at discharge scales with the neutron flux, that is to say the neutron power loading, whilst the activity at long times after irradiation scales with the neutron fluence.

4. Transmutations

Changes in composition of the alloys as a function of irradiation exposure are shown in Table 2. The table includes all solid transmutation

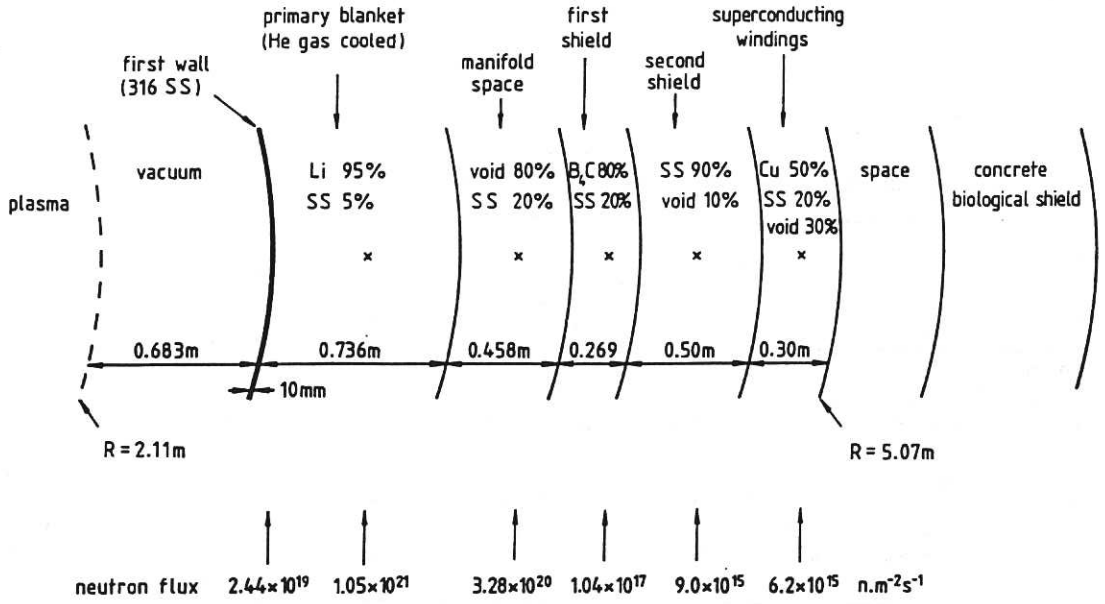

Figure 2 The blanket composition assumed for computational purposes.

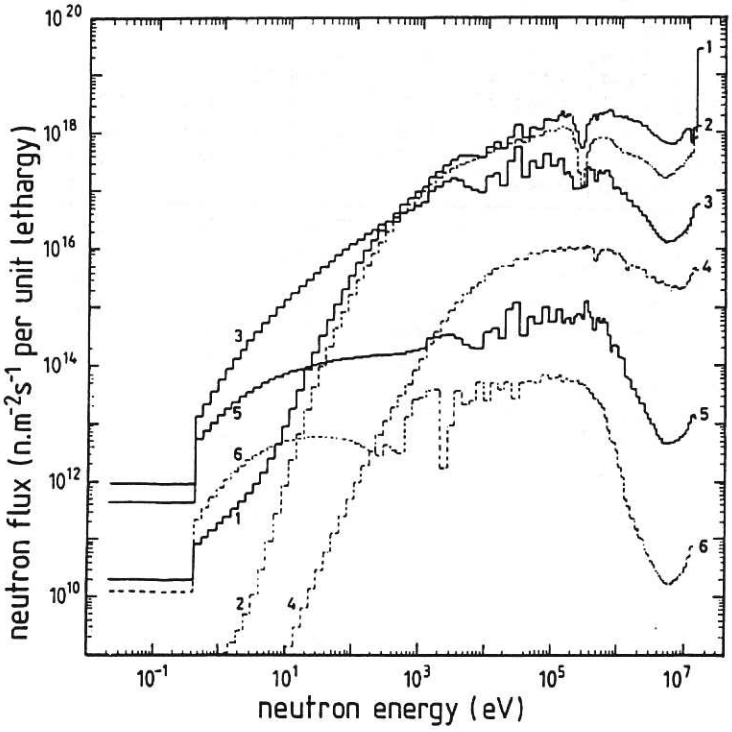

Figure 3 The neutron flux at various positions in the CCTRII blanket and shield.

1 first wall
2 centre of lithium breeder zone
3 manifold space behind breeding blanket
4 centre of first shield (B_4C)
5 centre of second shield (stainless steel)
6 centre of superconducting coils.

Table 2
Changes in alloy compositions under irradiation, excluding hydrogen and helium

Alloy	Element	Composition in mass percent										
		Number of year's exposure to neutron wall load of 7 MW m^{-2}										
		0	0.25	0.5	0.75	1.0	1.25	1.5	1.75	2.0	2.25	2.5
A	Cu	99.06	98.61	98.11	97.60	97.09	96.58	96.07	95.63	95.12	94.61	94.17
	Cr	0.8007	0.7997	0.7981	0.7971	0.7955	0.7940	0.7929	0.7914	0.7898	0.7888	0.7872
	Be	0.108	0.1078	0.1073	0.1070	0.1065	0.1062	0.1058	0.1054	0.1050	0.1045	0.1042
	Ni	–	0.3721	0.7433	1.113	1.481	1.848	2.213	2.576	2.938	3.298	3.656
	Zn	–	0.08766	0.1753	0.2623	0.3486	0.4343	0.5192	0.6035	0.6870	0.7701	0.8524
	Co	–	1.53 E-2	3.00 E-2	4.43 E-2	5.82 E-2	7.17 E-2	8.47 E-2	9.73 E-2	1.10 E-1	1.21 E-1	1.33 E-1
	V	–	9.04 E-4	2.08 E-3	3.27 E-3	4.45 E-3	5.63 E-3	6.80 E-3	7.96 E-3	9.12 E-3	1.03 E-2	1.14 E-2
	Ti	–	1.40 E-4	2.90 E-4	4.46 E-4	6.09 E-4	7.77 E-4	9.49 E-4	1.12 E-3	1.30 E-3	1.48 E-3	1.67 E-3
	Fe	–	1.26 E-5	4.78 E-5	1.05 E-4	1.84 E-4	2.87 E-4	4.13 E-4	5.63 E-4	7.37 E-4	9.37 E-4	1.16 E-3
B	Cu	99.50	99.00	98.49	97.85	97.47	96.96	96.52	96.01	95.50	95.06	94.55
	Cr	0.3016	0.3012	0.3006	0.3001	0.2996	0.2991	0.2986	0.2980	0.2975	0.2970	0.2965
	Zr	0.2007	0.2003	0.2000	0.1996	0.1992	0.1986	0.1985	0.1980	0.1977	0.1973	0.1969
	Ni	–	0.3990	0.7975	1.194	1.589	1.982	2.373	2.762	3.150	3.536	3.920
	Zn	–	0.08667	0.1733	0.2592	0.3445	0.4291	0.5131	0.5964	0.6788	0.7611	0.8422
	Co	–	1.55 E-2	3.06 E-2	4.51 E-2	5.92 E-2	7.30 E-2	8.62 E-2	9.91 E-2	1.12 E-1	1.24 E-1	1.35 E-1
	V	–	3.40 E-4	7.82 E-4	1.23 E-3	1.68 E-3	2.12 E-3	2.56 E-3	3.00 E-3	3.44 E-3	3.87 E-3	4.30 E-3
	Y	–	3.09 E-4	6.29 E-4	9.47 E-4	1.26 E-3	1.58 E-3	1.89 E-3	2.20 E-3	2.51 E-3	2.82 E-3	3.12 E-3
	Fe	–	1.32 E-5	5.00 E-5	1.10 E-4	1.93 E-4	3.00 E-4	4.32 E-4	5.89 E-4	7.72 E-4	9.81 E-4	1.22 E-3
	Ti	–	5.39 E-5	1.11 E-4	1.71 E-4	2.34 E-4	2.98 E-4	3.64 E-4	4.32 E-4	5.00 E-4	5.70 E-4	6.40 E-4
	Mo	–	1.05 E-5	3.97 E-5	8.00 E-5	1.25 E-4	1.71 E-4	2.18 E-4	2.65 E-4	3.12 E-4	3.58 E-4	4.04 E-4
	Sr	–	7.54 E-6	1.49 E-5	2.29 E-5	3.18 E-5	4.16 E-5	5.26 E-5	6.45 E-4	7.76 E-5	9.17 E-5	1.07 E-4
C	Cu	99.63	99.12	98.61	98.11	97.60	97.09	96.58	96.14	95.63	95.12	94.67
	O	0.1776	0.1773	0.1770	0.1768	0.1765	0.1762	0.1759	0.1756	0.1752	0.1751	0.1748
	Aℓ	0.1997	0.1992	0.1988	0.1983	0.1979	0.1975	0.1970	0.1966	0.1961	0.1957	0.1953
	Ni	–	0.3994	0.7981	1.195	1.591	1.984	2.376	2.765	3.154	3.540	3.925
	Zn	–	0.0867	0.1735	0.2595	0.3449	0.4297	0.5138	0.5971	0.6801	0.7618	0.8435
	Co	–	1.55 E-2	3.06 E-2	4.52 E-2	5.93 E-2	7.30 E-2	8.63 E-2	9.92 E-2	1.12 E-1	1.24 E-1	1.36 E-1
	Mg	–	3.93 E-4	7.86 E-4	1.18 E-3	1.57 E-3	1.96 E-3	2.35 E-3	2.74 E-3	3.12 E-3	3.51 E-3	3.89 E-3
	C	–	2.09 E-4	4.18 E-4	6.26 E-4	8.34 E-4	1.04 E-3	1.25 E-3	1.45 E-3	1.66 E-3	1.86 E-3	2.07 E-3
	Fe	–	1.32 E-5	5.01 E-5	1.20 E-4	1.93 E-4	3.00 E-4	4.33 E-4	5.90 E-4	7.73 E-4	9.83 E-4	1.22 E-3
	N	–	2.39 E-5	4.77 E-5	7.14 E-5	9.52 E-5	1.19 E-4	1.43 E-4	1.66 E-4	1.90 E-4	2.13 E-4	2.37 E-4
D	Cu	99.19	98.68	98.17	97.66	97.15	96.71	96.20	95.69	95.18	94.74	94.23
	Cr	0.5980	0.5969	0.5964	0.5954	0.5943	0.5933	0.5922	0.5912	0.5902	0.5891	0.5881
	Zr	0.2007	0.2003	0.2000	0.1996	0.1992	0.1989	0.1985	0.1980	0.1977	0.1973	0.1969
	Mg	0.0501	0.0501	0.0500	0.0500	0.0500	0.0500	0.0499	0.0499	0.0499	0.0499	0.0498
	Ni	–	0.398	0.794	1.19	1.58	1.98	2.37	2.75	3.14	3.52	3.91
	Zn	–	0.0863	0.173	0.258	0.343	0.428	0.512	0.595	0.677	0.759	0.840
	Co	–	1.55 E-2	3.05 E-2	4.50 E-2	5.91 E-2	7.27 E-2	8.59 E-2	9.88 E-2	1.11 E-1	1.23 E-1	1.35 E-1
	Y	–	3.09 E-4	6.29 E-4	9.47 E-4	1.26 E-3	1.58 E-3	1.89 E-3	2.20 E-3	2.51 E-3	2.82 E-3	3.12 E-3
	Ti	–	1.07 E-4	2.21 E-4	3.40 E-4	4.64 E-4	5.92 E-4	7.23 E-4	8.57 E-4	9.92 E-4	1.13 E-3	1.27 E-3
	Fe	–	1.32 E-5	4.99 E-5	1.09 E-4	1.92 E-4	2.99 E-4	4.31 E-4	5.88 E-4	7.70 E-4	9.78 E-4	1.21 E-3
	V	–	6.75 E-4	1.55 E-3	2.44 E-3	3.32 E-3	4.20 E-3	5.08 E-3	5.94 E-3	6.81 E-3	7.67 E-3	8.53 E-3
	Mo	–	1.05 E-5	3.97 E-5	8.00 E-5	1.25 E-4	1.71 E-4	2.18 E-4	2.65 E-4	3.12 E-4	3.58 E-4	4.04 E-4
	Sr	–	7.54 E-6	1.49 E-5	2.29 E-5	3.18 E-5	4.16 E-5	5.26 E-5	6.45 E-5	7.76 E-5	9.17 E-5	1.07 E-4

elements having final concentrations above 1 ppm by weight. The tabulated percentage mass values have been adjusted, where necessary, to account for changes in the effective atomic masses caused by deviations from the normal isotopic abundancies. The transmutation rates of the major constituent elements are roughly as indicated in Table 3. The generation rates of hydrogen and helium are given in Table 4, together with values calculated for type 316 stainless steel and the martensitic steel HT-9 under the same conditions of irradiation[12].

Table 3
Transmutation rates of principal elements in the MZC alloy as a function of exposure time at neutron power flux of 7 MW m^{-2}

Element	Concentration y (wt%) as function of irradiation time t in years
Cu	$y = 99.19 - 1.98t$
Cr	$y = 0.5980 - 0.00416t,\ t \geqslant 0.5$
Zr	$y = 0.2007 - 0.00150t$
Mg	$y = 0.0501 - 9.38 \times 10^{-5} t$
Ni	$y = 1.56t$
Zn	$y = 0.335t$
Co	$y = 6.24 \times 10^{-2} t - 3.42 \times 10^{-3} t^2$
Y	$y = 1.25 \times 10^{-3} t$
Ti	$y = 4.36 \times 10^{-4} t + 2.94 \times 10^{-5} t^2$
Fe	$y = 1.94 \times 10^{-4} t^2$
V	$y = 10^{-3} (3.49t - 0.2),\ t \geqslant 0.25$
Mo	$y = 10^{-4} (1.86t - 0.62),\ t \geqslant 0.75$
Sr	$y = 10^{-6} t (27.5 + 3.46t + 1.08t^2)$

Table 4
Rates of generation of hydrogen and helium per 1 MWy m^{-2} neutron power fluence

Alloy	Hydrogen (appm)	Helium (appm)
A	703	108
B	704	105
C	704	111
D	703	105
316 SS	723	157
HT–9	551	146

The dominant effect in all of the selected alloys is the transmutation of the copper base, which essentially overshadows any differences between the individual alloys. Over the assumed irradiation exposure approximately 5% of the copper component is transformed into other elements, principally nickel at up to 3.9% and zinc to 0.8% together with lesser proportions of cobalt, vanadium, titanium, iron and yttrium. Natural copper consists of the two isotopes Cu^{63} and Cu^{65}, with relative abundancies of 69.1% and 30.9%, respectively. For the present first wall spectrum the principal group-averaged cross-sections for copper given by UKCTRIIIA are as shown in Table 5. For both isotopes the predominant reaction is (n,2n) which leads to the generation of Ni^{62} and Ni^{64} in the abundance ratio of about 2:1. The rate of generation of nickel through (n,2n) reactions would be less in regions of the blanket where the neutron spectrum is softer or in blanket designs employing water as the coolant.

Table 5
Principal group-averaged cross sections for copper used in UKCTRIIIA

Reaction	Cross Section (barns) Cu^{63}	Cu^{65}
(n, 2n)	0.116	0.204
(n, p)	0.036	5.2×10^{-3}
(n, α)	9.5×10^{-3}	4.4×10^{-3}
(n, nα)	2.4×10^{-3}	2.5×10^{-3}
(n, γ)	0.049	0.023

Nickel is completely soluble in the copper lattice whilst zinc is soluble up to a limit of 37% at 350^0C, hence the relatively low concentrations of these elements generated by the transmutations should not result in any phase changes in the alloys. Assuming that they pass into solid solution, both elements can be expected to increase plastic flow stresses up to moderately elevated temperatures. These additions are, however, likely to cause a substantial reduction in the thermal conductivity and the magnitude of this effect is estimated in the following section.

5. Effect of transmutation elements on the thermal conductivity

On the assumption that the transmutation elements enter into solid solution with the host material, their influence on the conductivity can be estimated by means of the Wiedemann-Franz law and the solid solution resistivity coefficients of the elements generated. The electrical resistivity ρ of a dilute binary alloy is represented approximately by the equation[13]:

$$\rho \simeq \rho_o + X\, y_x$$

where ρ_o = electrical resistivity of the host material
X = mole fraction of solute element present
y_x = solid solution resistivity coefficient of the solute element

According to the Wiedemann-Franz rule the electrical resistivity and the thermal conductivity k are related through the equation:

$$\frac{k\rho}{T} = \text{a constant}$$

where T is the absolute temperature. This relationship is not exact, however, and has been refined by Smith and Palmer[14] to give an equation of the form:

$$k = \frac{LT}{\rho} + k_o$$

in which L is the Lorenz number, 2.44×10^{-8} $W\Omega K^{-2}$, and k_o is a constant conductance term of the order 5 $Wm^{-1}K^{-1}$. Copper alloys obey this rule quite closely at room temperature and above.

Table 6
Effect of solute elements on the room temperature electrical and thermal conductivities of pure copper

Element	Electrical Resistivity Coefficient $\mu\Omega m/wt\,\%$	Thermal Conductivity for 1% wt of solute $Wm^{-1}\,K^{-1}$
Zn	0.0027	367
Ni	0.0128	246
Sn	0.0157	224
Aℓ	0.0288	161
Si	0.0666	90
P	0.138	51
Ti	~0.28	29

Table 6 gives published[15-17] values of the room temperature electrical resistivity coefficient for various solute elements in pure copper, together with the corresponding thermal conductivity coefficient calculated from the Smith-Palmer relationship. It is seen from the table that, in comparison with some other elements, the two principal solid transmutation products nickel and zinc are not particularly potent in

reducing the conductivity. Figure 4 gives a rough indication of the influence of nickel and zinc in solid solution on the room temperature thermal conductivity of pure copper, as deduced from the Smith-Palmer relation and the experimental data given by Ho et al[5]. The concentrations of 3.9% Ni and 0.8% Zn predicted to be generated over the notional lifetime exposure of 17.5 $MWym^{-2}$ are thus estimated to reduce the thermal conductivity of the alloy by about a factor 3.6. It will be noted, moreover, that the rate of diminution of the conductivity is most rapid at the beginning of the irradiation period.

Whilst the degraded conductivity would still be a factor 5 or so higher than that of type 316 stainless steel, for example, it is evident that the perceived advantage of the copper alloy would be much reduced during its service life and it therefore appears worthwhile to seek some way of nullifying the effects of the transmutation products. One possible approach might consist of introducing into the alloy an element possessing a strong affinity for nickel and which would remove it from solution through the formation of an intermetallic compound. Plausible additions might be Aℓ, Si, P, Sn and Ti, which can form compounds such as $Ni_3Aℓ$,

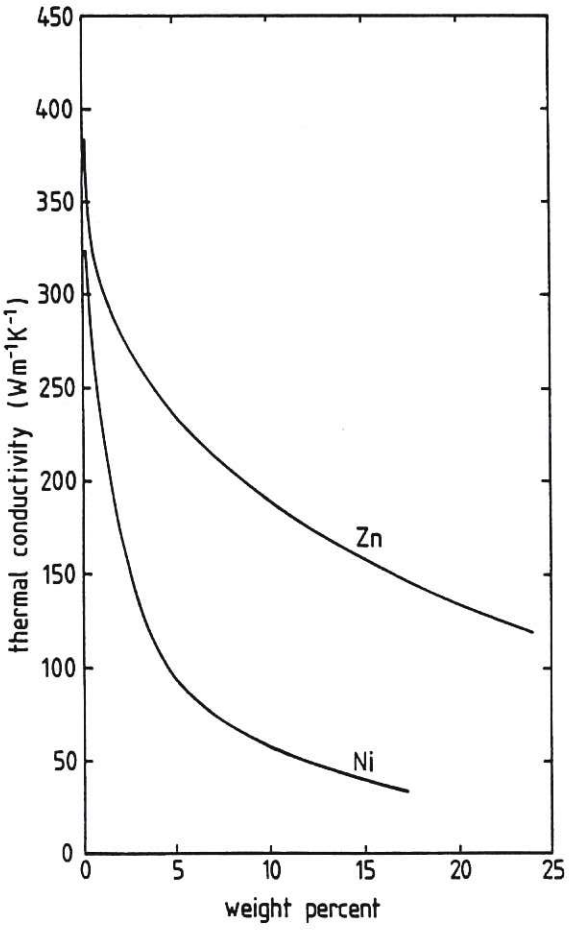

Figure 4 Effect of nickel and zinc on the room temperature thermal conductivity of copper.

Ni_2Si, Ni_3Sn, Ni_3Ti and NiCuTi. Some of these compounds are already utilised as precipitation-hardening agents in copper alloys. Unfortunately, all of these elements cause a greater reduction in conductivity than does nickel itself and, since they would need to be added at a concentration around 1% at the outset, the overall effect of the thermal conductivity over the component lifetime would not be beneficial. Neither does it appear possible, from an examination of the pertinent nuclear cross-sections, to incorporate a benign element that would be transmuted to a nickel-scavenging element at a rate commensurate with that of the nickel generation.

6. Induced radioactivity

Since the radioactivity induced in the alloys under consideration is dominated by that of the copper component there are only minor variations in the activation characteristics of the selected alloys. Thus the curve shown in Fig. 5 for the CuCrZrMg (MZC) alloy can be taken as representative of the group. The contribution from individual radionuclides is indicated by plotting a single point at a level corresponding to its activity at the cessation of irradiation and at a time value corresponding to its decay half life. To allow comparison with well-known materials the figure also includes curves for type 316 stainless steel and the martensitic steel HT-9, for identical conditions of exposure[12].

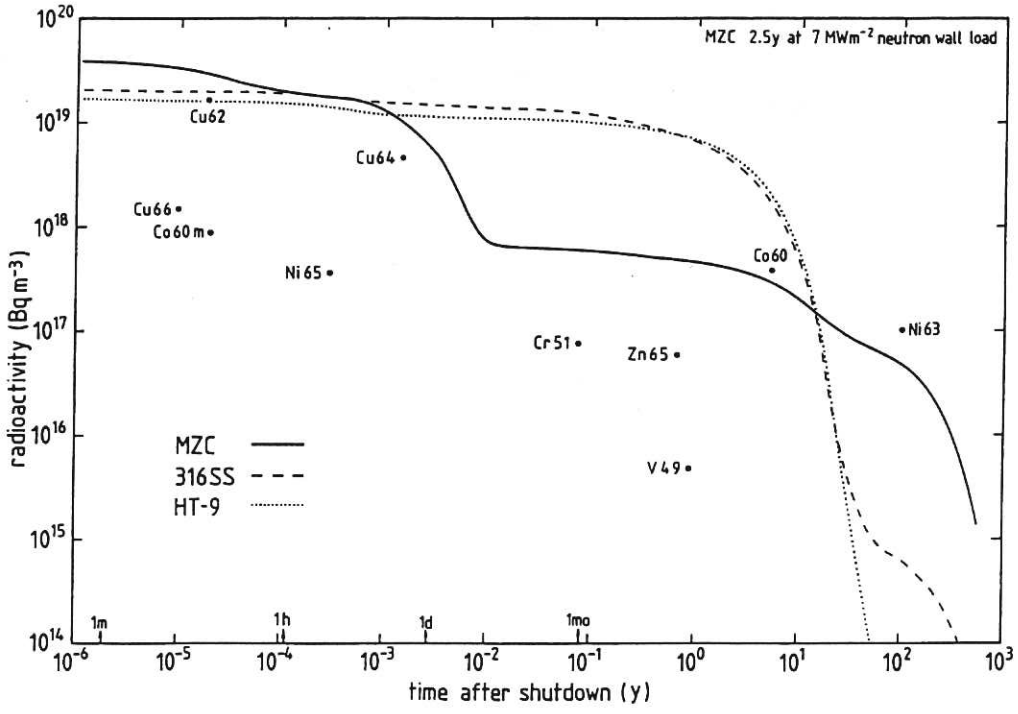

Figure 5 Decay of radioactivity with time for MZC and the reference steels AISI316 and HT-9.

At shutdown the specific radioactivities of the copper alloys are about a factor 2 higher than those of the steels and are mainly due to the shortlived isotopes Cu^{62} and Cu^{64}, with respective half lives of 9.8m and 12.7h. A few days after shutdown the activity of the copper alloy falls by about a factor 50 whilst that of the steels hardly changes. The activity of the copper alloy remains about an order of magnitude lower than those of the steels for up to 5 years. Between 20 and 1000 years, however, the copper alloys retain a relatively high activity, mainly associated with the decay of Ni^{63} with a half life of 100y, though the activity diminishes by six orders of magnitude between 100y and 3000y. It remains nearly constant at around 5×10^{10} Bqm^{-3} between 3×10^{3}y and 10^{5}y, owing to the decay of Fe^{60}, before any further decrease. For comparison, the most favourable iron-based alloys exhibit a plateau in their decay characteristic at about 10^{12} Bqm^{-3} between 300y and 10^{6}y, due to the activity from Mn^{53}[6].

7. Surface γ dose rate

The computed γ dose rates at the surface of a large thick slab of MZC alloy and of the reference steels are shown as a function of time in Fig. 6. The dose rates for all three materials are comparable during the first year following irradiation. The copper alloy and 316 steel have

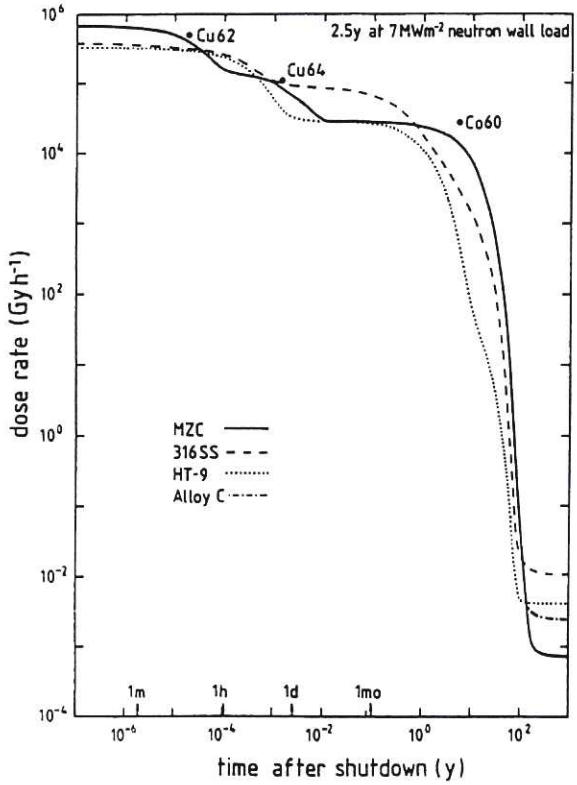

Figure 6 Decay of dose rate with time for MZC, Alloy C and the reference steels.

similar rates up to about 100 years whilst that for HT-9 is one to two orders of magnitude lower during this time. After about 200 years the dose rate for the copper alloys levels out near 10^{-3} Gyh^{-1}, at which it remains essentially constant for 10^5 years as a result of the $Fe^{60} \rightarrow Co^{60}$ β-decay reaction.

The dose rate curves given in Fig. 1 show that aluminium exhibits a dose rate 10^3 times that of copper during the period 10^2 to 10^5 y after irradiation. The activity of the aluminium is associated with the gamma decay of $^{26}A\ell$, characterised by a high-energy γ emission of 1.8 MeV and a half life of 7.4 x 10^5 y. Since the alumina-strengthened alloy considered in this study (alloy C of Table 1) has an aluminium content of about 0.2% by mass, it follows that the contribution from the aluminium component will dominate the long-term dose rate of this alloy.

8. Afterheat

The amount of heat generated in a material by nuclear decay processes following reactor shutdown determines the provisions that must be made for the cooling of reactor components during off-duty periods of reactor operation and for the cooling of expired components during and after their removal from the reactor. The afterheat decay characteristics of MZC and the reference steels are given in Fig. 7. The major radio-nuclides

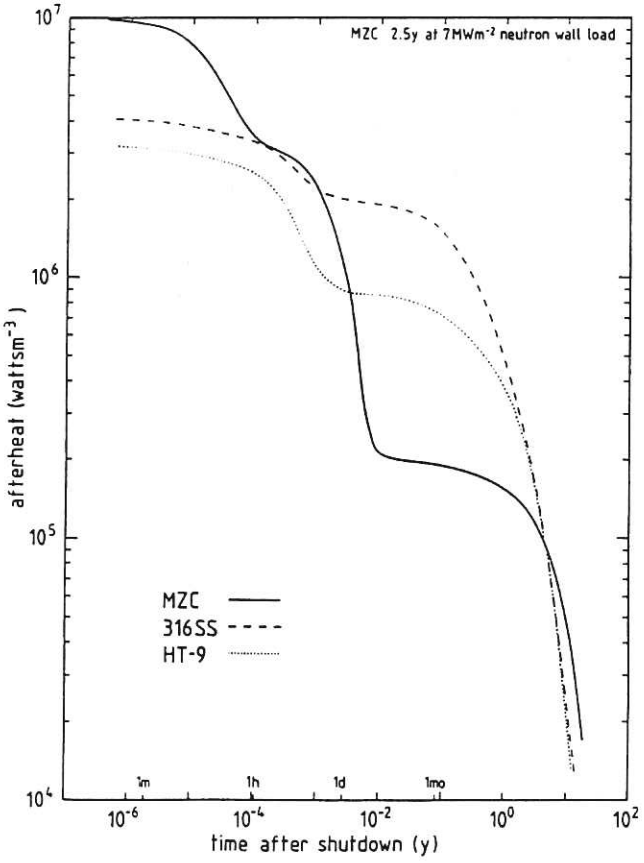

Figure 7 Time dependence of the nuclear afterheat.

contributing to the afterheat in the copper based alloys are Cu^{62}, Cu^{64}, Cu^{66}, Co^{60} and Co^{62}. The afterheat level at shutdown represents 1.4%, per centimetre wall thickness, of the operating first wall neutron power loading and it remains close to this level for several minutes after shutdown. Initially the copper alloy has a heat generation rate about three times greater than those of the steels but after about a day and over a subsequent period of at least a year it falls well below the rates for the steels and remains at a lower level for up to 5 years after discharge.

9. Biological hazard potential

Figures 8 and 10 show the computed biological hazard potential indices for air and water dispersal of the MZC alloy as a function of time after irradiation. Corresponding curves for the steels are given in Figs. 9 and 11. It is seen that for both air and water dispersal Co^{60} is the main source of hazard in the short term, that is to say up to about 10 years, whilst Ni^{63} is almost entirely responsible for the long term hazard. Initially the copper alloy has a BHP_a value similar to that of HT-9 and marginally lower than that of 316 steel. In the longer term, around 100 years, for which the BHP for water dispersal is more relevant, the Ni^{63} content of the copper alloy maintains the BHP_w value at a relatively high level compared with those of the steels.

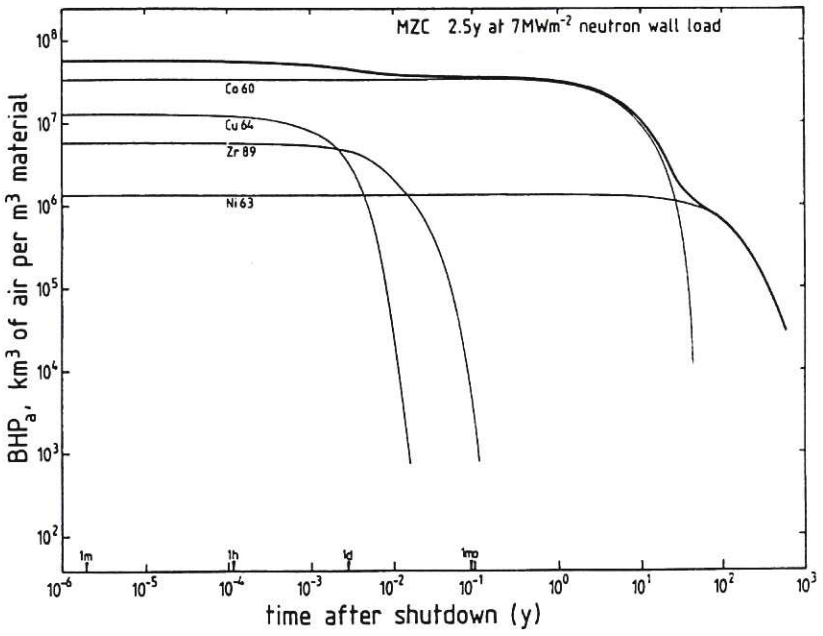

Figure 8 Time dependence of the biological hazard potential for air dispersal of MZC.

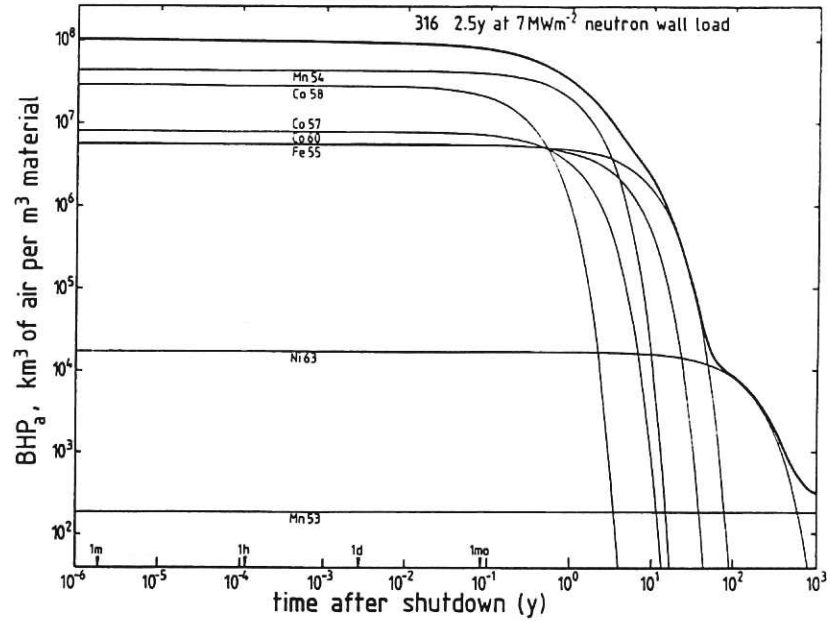

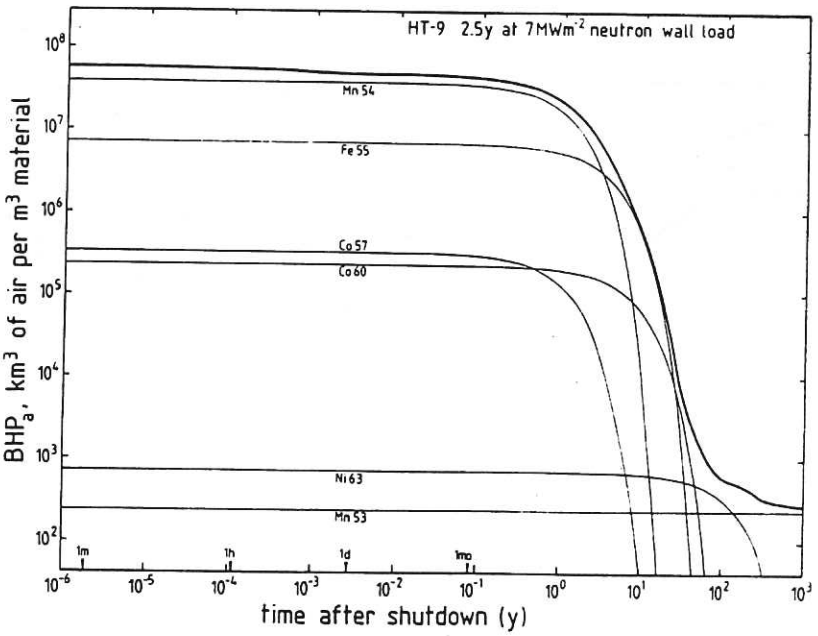

Figure 9 Time dependence of the biological hazard potential for air dispersal of the reference steels.

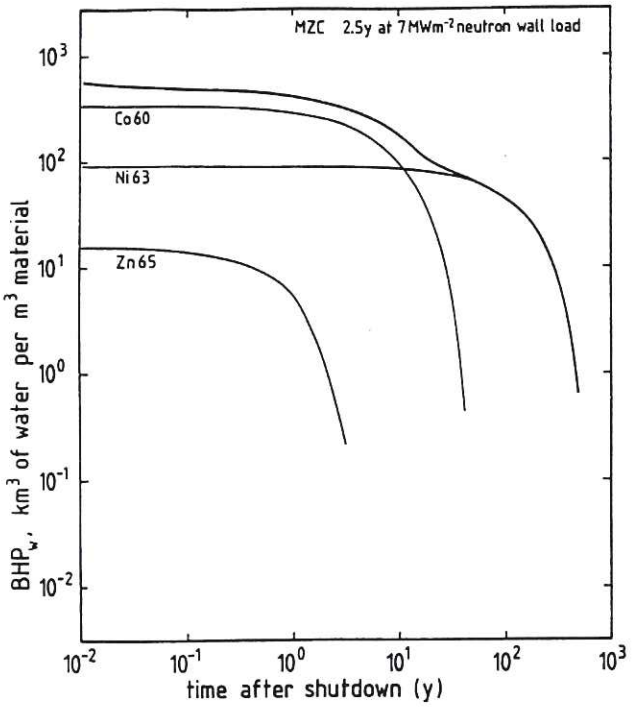

Figure 10 Time dependence of the biological hazard potential for water dispersal of MZC.

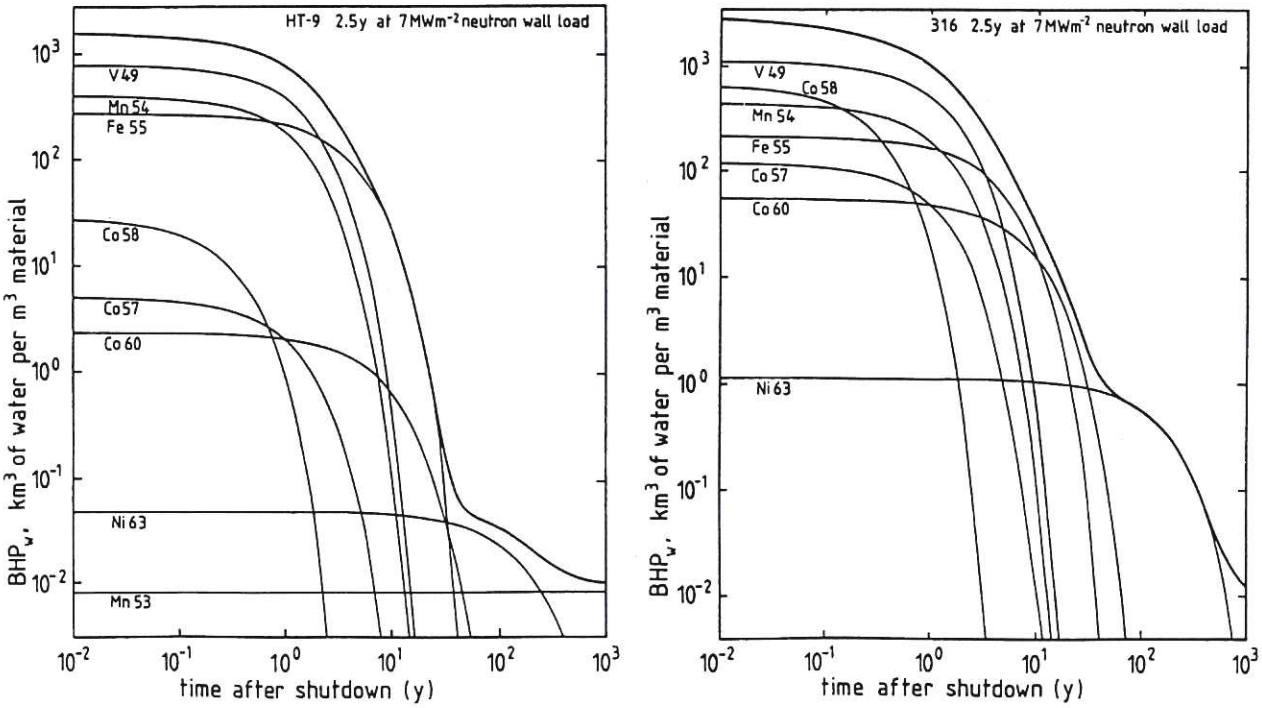

Figure 11 Time dependence of the biological hazard potential for water dispersal of the reference steels.

10. Effect of impurity elements

The results presented so far apply to the copper alloys in a chemically-pure state. The unintended impurity elements inevitably present in real materials can have significant effects on their activation properties. Whilst the representative alloy MZC is not normally assayed for minor impurities the impurity content of the copper component would generally be expected to be similar to that of oxygen-free high-conductivity (OFHC) copper, which is used as a starting material in the preparation of the alloy. A typical trace element analysis quoted by Amax Copper, Incorporated for their OFHC brand copper is given in Table 7. An ORIGEN computation was performed for MZC containing these elements at concentrations corresponding to the upper limits indicated in the table. The results showed the impurities to have a relatively minor effect on the radioactivity, afterheat and biological hazard potential but a pronounced influence on the dose rate, as is illustrated by Fig. 12. It should be noted, however, that the contributions from As, Bi, Te and Se are not included, since the cross section library used does not contain data for these elements. At the residual concentration of 20 ppm typical of highly-refined coppers, silver increases the dose rate by as much as a factor 40 in the period between 100and 1000years after irradiation. It follows that the silver content of copper alloys should be maintained below about 1 ppm to avoid a significant increase in the total dose rate. Silver is usually the main impurity in commercial coppers and 15 ppm represents about the lowest concentration normally attained in the industrial production of electrolytically-refined copper. There is in fact little incentive to reduce the silver content of commercial alloys below this level, since the presence of silver is not detrimental in most applications. Nevertheless, methods of reducing the residual silver content could probably be developed if justified by a particular requirement.

Table 7
Typical trace element analysis of AMAX brand OFHC copper

Element	Concentration (ppm)	Element	Concentration (ppm)
S	10–15	Fe	2–3
Ag	12–20	Mn	0.2
As	1–3	Hg	< 1
Pb	3–7	Cd	< 1
Sn	1–2	Zn	< 1
Ni	4–8	P	< 3
Sb	4–8	Se	1–3
Bi	0.2–0.8	O	< 0.3
Te	< 2		

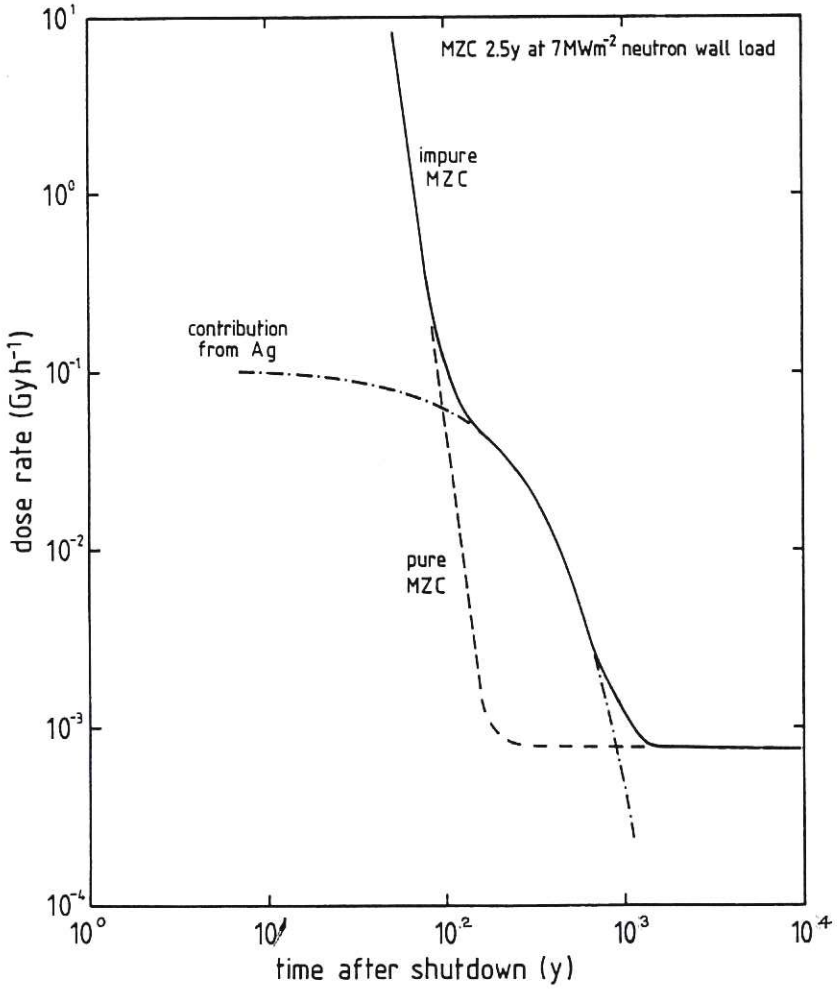

Figure 12 Effect of the impurities indicated in Table 7, notably 20 ppm silver, on the dose rate of alloy MZC.

Because of their dilution by the copper base, the impurities introduced via the alloying additions such as chromium and zirconium will generally have only a minor effect on the activation of the alloys. Aluminium, which exhibits a relatively high dose rate in the interval 10^2 to 10^5 years after irradiation (Fig. 1) may be present at concentrations up to about 2000 ppm in chromium obtained by pyrometallurgical routes, though electrolytic purification can be employed to prepare chromium free from significant concentrations of radiologically-troublesome impurities. Moreover, as reference to Fig. 1 shows, the aluminium component will only increase the long-term dose rate noticeably if it is present at a level exceeding 1000 ppm in the final alloy.

The other principal alloying addition, zirconium, can be produced on a commercial scale in a fairly pure state and typical analyses of reactor-

grade zirconium, as used in the manufacture of Zircalloy, reveal no radiologically-significant concentrations of impurities.

11. Discussion and conclusions

On the basis of their thermal and mechanical properties in the unirradiated condition, high-performance copper alloys are attractive materials for fusion reactor components subjected to high pulsed heat loads and operating at temperatures up to about 350^0C. Very little information on their radiation damage response under fusion conditions exists at present, however, and it remains to be established whether adequate strength and ductility are retained at elevated temperature and under fusion neutron bombardment.

The present study indicates that the copper base of an alloy exposed to a first wall neutron flux will be transmuted at a rate of about 0.28 wt % per $MWym^{-2}$, the principal daughter elements being nickel and zinc, both of which are soluble in the host lattice. In the dilute alloys considered here the foreign atoms thus introduced are expected to cause a substantial diminution of the electrical and thermal conductivities. Zinc is much less potent than nickel in this respect and its influence in reactor components might be further diminished through its tendency to volatilise under conditions of high vacuum and elevated temperature. It is estimated that the thermal conductivity would be reduced by about a factor 4 during an exposure to 17.5 $MWym^{-2}$ neutron power fluence. Even with such a reduction, however, the conductivities of the copper alloys will still be many times greater than those of stainless steels, for example, so the detrimental effect of transmutations does not necessarily rule out the use of copper alloys for high heat flux applications. Moreover, it may prove possible in the future to develop compositions in which the transmutation products are accommodated with minimal adverse effect on the alloy properties.

In the absence of impurity elements the radiological behaviour of the alloys studied is almost entirely governed by the induced activity of the copper base. The short-term activity decay characteristics are found to be generally comparable with and in some respects more favourable than those of the reference steels considered. In the longer term, beyond about 100 years, on the other hand, the radionuclides Co^{60} and Ni^{63} in the copper alloys give rise to relatively high activities, dose rates and biological hazard potentials. Although aluminium is present only at low concentration in the alumina dispersion strengthened alloys, it will generally make a dominant contribution to their long-term dose rate beyond about 200 y after irradiation.

Whereas the remanent activity of some alloys systems, such as the commercial stainless steels, might be substantially reduced through either

elemental substitution or isotopic tailoring this possibility does not exist in the case of the copper alloys since the activity primarily arises from the copper base itself. The compositional simplicity of the copper-based alloys may, however, permit chemical reprocessing of active waste material to be considered. It will in any case be essential to strictly limit the allowed concentrations of impurity elements such as silver, which would otherwise give rise to unacceptably high levels of long-term activity.

12. Acknowledgements

The author wishes to thank O N Jarvis, B H Patrick and M G Sowerby for helpful discussions and assistance in performing the computations.

13. References

1. O.K. Harling, G.P. Yu, N.J. Grant and J.E. Meyer, Application of high strength copper alloys for a fusion reactor first wall, J. Nucl. Mater. 103-104 (1981) 127.

2. G.W. Cort, A.L. Graham and K.E. Christensen, A high-flux first wall design for a small reversed-field pinch reactor, LA-UR-82-220 (1982).

3. P.I.H. Cooke and R.A. Krakowski, The advantages and disadvantages of high-power-density fusion: first wall thermo-mechanical limits, to be published as a Culham Laboratory Report.

4. A. Caie and G.J. Butterworth, A study of the application of a high-strength copper alloy for the first wall of a high-heat-flux fusion reactor, Proc. 13th Symposium on Fusion Technology, Varese, 24-28 September 1984.

5. C.Y. Ho, M.W. Ackerman, K.U. Wu, S.G. Oh and T.N. Havill, Thermal conductivity of ten selected binary alloy systems, J. Phys. Chem. Ref. Data 7 (1978) 959.

6. O.N. Jarvis, Selection of low-activity elements for inclusion in structural materials for fusion reactors, AERE-R10496, June 1982

7. O.N. Jarvis, Low-activity materials: Reuse and disposal, AERE-R10860, March 1983.

8. J.T.D. Mitchell and A. Hollis, A tokamak reactor with servicing capability, Proc. 9th Symp. on Fusion Technology, Garmisch-Partenkirchen, Sept 1976, Pergamon Press.

9. O.N. Jarvis, Transmutation and activation of fusion reactor wall and structural materials, AERE-R9298, Jan 1979.

10. O.N. Jarvis, Description of the transmutation and activation data library UKCTRIIIA, AERE-R9601 (revised).

11. M.J. Bell, ORIGEN - The ORNL isotope generation and depletion code, ORNL-4628 (1973).

12. G.J. Butterworth and O.N. Jarvis, Comparison of transmutation and activation effects in five ferritic alloys and AISI 316 stainless steel in a fusion neutron spectrum, Third Topical Meeting on Fusion Reactor Materials, Albuquerque, New Mexico, Sept 1983.

13. L.H. Van Vlack, Materials Science for Engineers, Addison-Wesley, London, 1970.

14. T.W. Watson and D.R. Flynn, Thermal conductivity and electrical resistivity of beryllium copper foil, Trans. Met. Soc., AIME 242 (1968) 876.

15. K. Dies, Kupfer and Kupferlegierangen in der Technik, Springer-Verlag, Berlin, 1976.

16. A.K. Nikolaev, I.F. Pruzhinin and V.M. Rozenberg, Sov. J. of Non-Ferrous Metals 17 (1976) 85.

17. A.R. Bailey, A Textbook of Metallurgy, Macmillan and Co., London, 1954, p280.